RSC Advances

PAPER

View Article Online
View Journal | View Issue

Cite this: *RSC Adv.*, 2021, **11**, 22993

A novel carbon dot/polyacrylamide composite hydrogel film for reversible detection of the antibacterial drug ornidazole

Weizhen Wu,†[a] Xiaoyi Wu,†[ab] Miao He,[a] Xiaolin Yuan,[a] Jiaping Lai *[a] and Hui Sun*[b]

Received 23rd February 2021
Accepted 15th June 2021

DOI: 10.1039/d1ra01478a

rsc.li/rsc-advances

A carbon dot/polyacrylamide (CDs/PAM) composite hydrogel film with stable fluorescence performance was fabricated by merging a hydrogel film and carbon dots (CDs) with blue fluorescence, which were prepared by hydrothermal synthesis using anhydrous citric acid and acrylamide as carbon sources. The obtained CDs/PAM composite hydrogel film exhibited a good fluorescence quenching effect on ornidazole (ONZ), and can be used for the quantitative detection of ONZ. In the ONZ concentration range of 5–60 μM, a good linear relationship between the fluorescence quenching efficiency of the CDs/PAM composite hydrogel film and the concentration of ONZ solution was obtained with a low detection limit of 2.35 μM. In addition, the detection system has good selectivity and strong anti-interference capacity, and can be used in repeated cycles for detection.

1. Introduction

Ornidazole (ONZ) is a 5-nitroimidazole derivative and is commonly used in the prevention and treatment of infectious diseases caused by susceptible protozoa and anaerobic bacteria.[1] ONZ has similar activity to other nitroimidazole drugs, while ornidazole is more preferred in some clinical treatments due to its longer half-life and lower dose requirement to achieve the same effect. However, ornidazole has certain side effects, including genotoxicity, genomic instability, damage to the central nervous system, and autoimmune hepatitis induced by the drug. Long term use of ONZ will cause harm to the health of the users.[2–4] The quality control of the drug and the monitoring of ornidazole residues in the human body are of great necessity. Thus, detection of ornidazole is needed. According to the current reports, the methods for detecting ornidazole mainly include high performance liquid chromatography, high performance thin layer chromatography, liquid chromatography-tandem mass spectrometry, *etc.*[5–7] None of these methods can achieve wide application due to their high cost, complex pre-treatment operation and the need of professional technicians. To overcome the shortcomings above, fluorescence analysis method was applied to detect ONZ with high sensitivity, good stability, simple pre-treatment process and convenient operation. The fluorescence detection method has a good application prospect in the future and great possibility to become one of the mainstream method of detecting actual environment samples. Therefore, it is of great practical value to detect ONZ by fluorescence analysis.

Hydrogel, a three-dimensional network of hydrophilic polymers, can swell in water and hold a large amount of water while maintaining the structure due to chemical or physical cross-linking of individual polymer chains. Hydrogels not only have certain flexibility, but also have special biocompatibility.[8,9] In recent years, some nanocomposite hydrogels have been developed, such as graphene composite hydrogels, carbon nanotube composite hydrogels, *etc.*, which have improved the poor mechanical properties in the past.[10–13] As a new kind of carbon nanomaterial with fluorescent, carbon dots (CDs) has been broadly used in the field of chemistry, leading to research findings that the material show excellent properties, such as excellent luminescent properties, good water-solubility, fluorescence stability and biocompatibility. CDs has been widely used in cell imaging,[14–17] photocatalysis,[18] electrocatalysis,[19] chemical sensor and probes[20–25] and other fields.[26,27]

Same as other nanomaterials such as graphene and carbon nanotubes, CDs has rich active groups on its surface. Therefore, based on these similar properties, CDs also have great potential in preparing composite hydrogels.[28] Comparing with pure carbon dots, one great advantage of carbon dots composite hydrogel film is that it can be fixed and used circularly. Thus, it is of great importance to develop a new CDs composite hydrogel film for fluorescence sensor detection. So far, no research has reported the application of CDs composite hydrogel film in ONZ detection. In this work, the CDs/PAM composite hydrogel film was successfully prepared and used for detection of ONZ.

[a]*School of Chemistry, South China Normal University, Guangzhou 510006, China. E-mail: laijp@scnu.edu.cn*

[b]*College of Environmental Science & Engineering, Guangzhou University, Guangzhou 510006, China. E-mail: esesunhui@gzhu.edu.cn*

† Weizhen Wu and Xiaoyi Wu contributed equally to this work.

2. Experimental

2.1 Materials and reagents

Ornidazole, 2-methylimidazole, 4-imidazolecarboxaldehyde, anhydrous citric, glucose, urea were purchased from Aladdin Reagent Co., Ltd. (Shanghai, China). Acrylamide was received from Damao Chemical Reagent Co. Ltd (Tianjin, China). L-Histidine, L-serine, L-lysine, L-glutamic acid were purchased from Dalian Meilun Biotechnology Co., Ltd (Dalian, China). *N*,*N*-Methylenebisacrylamide bis-acrylamide, ammonium persulfate were received from Makclin Biochemical Co. Ltd. (Shanghai, China). *N*,*N*,*N*′,*N*′-Tetramethylethylenediamine was obtained from Bailingwei Technology Co. Ltd. (Beijing, China).

2.2 Equipment

The drying oven (DHG-9070A) was purchased from Shanghai Yiheng Scientific Instrument Co., Ltd. The analytical balance (FA2004B) was purchased from Techcomp Precision Balances (Shanghai) Co., Ltd. The fluorescence spectrophotometer (FL-4600) was purchased from Hitachi, Japan. The magnetic stirrer (JK-MSH-Pro) and the pH meter (PHS-3C) were purchased from Shanghai Jingke Scientific Instrument Co. Ltd. The 50 μL/100 μL/1000 μL/5 mL pipette gun were purchased from DLAB Scientific Co., Ltd. The microfiltration membrane (0.22 μm) was purchased from Jinteng microfiltration membrane.

2.3 Synthesis of CDs

The CDs were prepared by a modified hydrothermal carbonization method.[29–31] In brief, 1 g acrylamide (AM) and 0.5 g anhydrous citric were dissoved in 10 mL of deionized water, and stirred for 5 min to form a homogeneous solution. Then the above solution was transferred into a 25 mL poly-tetrafluoroethylene stainless steel reactor, and heated in an oven at 180 °C for 6 h. After cooling to room temperature naturally, the CDs containing suspensions was filtered with a 0.22 μm filter membrane to remove the large particles. Subsequently, the filtrate was dialyzed for roughly 24 h through a dialysis bag with MWCO of 1000 Da, which can purify the CDs solution. Finally, the pure CDs solution was stored in the refrigerator for future use.

2.4 Preparation of CDs/PAM composite hydrogel films

The CDs/PAM composite hydrogel films were synthesized based on the previously reported procedures,[32–34] and the preparation process is shown in Scheme 1. Firstly, 1 g acrylamide (AM) and 30 mg *N*,*N*-methylenebisacrylamide bis-acrylamide (MBA) were dissoved in 10 mL deionized water, then 300 μL pure CDs solution were added in the solution. After ultrasonic dispersion for 15 min, 12 mg ammonium persulfate (APS) and 10 μL *N*,*N*,*N*′,*N*′-tetramethylethylenediamine (TMEDA) were added to the mixture and continuously stirred for another 5 min. Then the reaction solution was quickly poured into the 1 mm gap between a piece of glass (1.3 cm width × 5 cm length) and a piece of polyethylene terephthalate (PET) film (1.3 cm width × 3 cm length). Placed at room temperature for 2 h, the CDs/PAM composite hydrogel films were prepared on the quartz glass slide by radical polymerization. In order to remove the unreacted molecures, the composite hydrogel films were washed with deionized water. Finally, the product was further immersed in phosphate buffer solution of pH 7 to achieve swelling equilibrium.

2.5 Procedure for fluorescence detection of ONZ

The CDs/PAM composite hydrogel film in aquous solution with a certain concentration of ONZ was placed in the cuvette and aligned with the excitation beam. The fluorescence spectra were recorded by the Hitachi FL-4600 fluorescence spectrophotometer with the excitation wavelength being set at 320 nm. The emission slits and excitation slits were set at 10 nm, the voltage of the photomultiplier was set at 400 V.

2.6 Detection of ONZ in real samples

In order to verify the applicability of the proposed method in real sample analysis, we further applied the method to detect ONZ in human urine samples and ONZ tablets. The human urine samples were filtered and spiked with a series concentrations of ONZ. The ornidazole dispersible tablets were purchased from local pharmacies. They were sonicated in an appropriate amount of absolute ethanol before testing. Finally, 8 μM ONZ solution was prepared and determined directly and by standard addition recovery method, seperately.

3. Results and discussion

3.1 Characterization

3.1.1 Characterization of CDs. In order to characterize the morphology, structure and composition of the synthesized CDs,

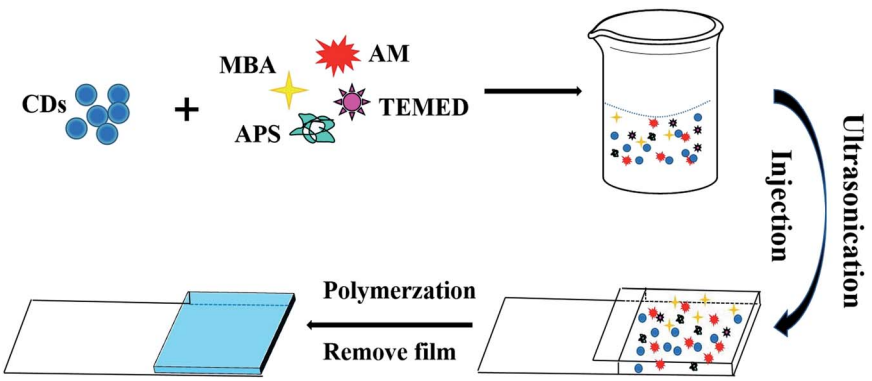

Scheme 1 Schematic diagram of CDs/PAM composite hydrogel film preparation.

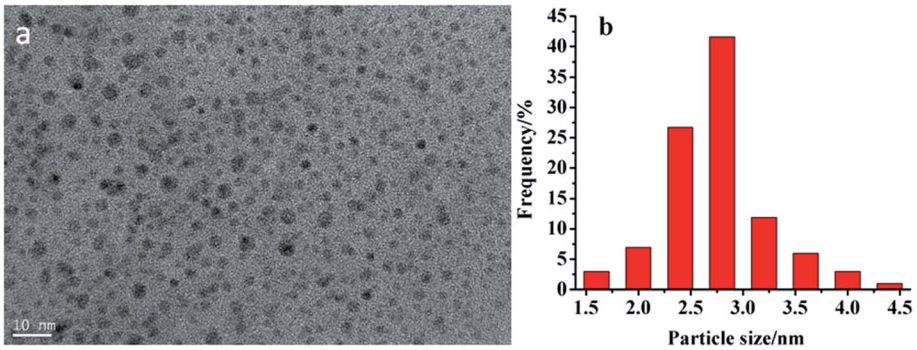

Fig. 1 Morphological characterization of CDs ((a): TEM image of the CDs; (b): size distribution of CDs).

TEM image, Fourier transform infrared (FTIR) spectrum and X-ray powder diffractometry (XRD) were used. The results show that the CDs are approximately round shape, and appear uniform morphology (Fig. 1a). The average particle size of the CDs counted by particle size distribution software are about 2.75 nm (Fig. 1b).

The Fourier transform infrared (FTIR) spectrum was used for the analysis of CDs, on the surface of which the existence of bonded hydrophilic functional groups is to be determined. The spectra is recorded in the range of 4000–1000 cm^{-1}. The results (Fig. 2a) show that the broad peaks at 3197 cm^{-1} and 2935 cm^{-1} are caused by the stretching vibration of N–H and C–H, respectively,[35] and the broad peaks at 1694 cm^{-1} and 1543 cm^{-1} are attributed to the asymmetric stretching of C=O and N–H, respectively. Peaks at about 1445 cm^{-1} and 1163 cm^{-1} also indicate the existence of C–N and C–O.[36] The existence of these absorption peaks indicates that the surface of CDs contains a large number of hydrophilic active groups such as carboxyl and amino groups.

To explore the surface element composition of the CDs, the structure of CDs was characterized by X-ray powder diffractometer (XRD). The results are shown in Fig. 2b. A broad diffraction peak appeared near 22.8°, proving that the carbon in the quantum dots are mainly amorphous.

The CDs powder was prepared by freeze-drying the purified CDs and then characterized by XPS. The full-spectrum scanning was shown in Fig. 3a. It can be clearly seen that the elemental peaks appear at 288.68 eV, 399.88 eV, and 531.68 eV, corresponding to C 1s, N 1s, O 1s, and the contents are 62.96%, 6.57%, and 30.48%, respectively.[37] The high resolution C 1s spectrum in Fig. 3b exhibits three peaks at 284.7 eV, 285.3 eV, and 288.5 eV, corresponding to C–C/C=C, C–N, C=O, respectively.[38] The N 1s spectrum in Fig. 3c shows 2 peaks at 399.8 eV and 401.1 eV, revealing that nitrogen exists in the forms of pyrrolic-like N and N–H.[39] The peaks observed at 531.6 and 533.0 eV in the O 1s spectrum (Fig. 3d) demonstrate that oxygen atoms are present in the forms of C=O and C–O, respectively.[40,41] This further proves that the surface of CDs is rich in active groups such as carboxyl and amino groups.

The quantum yield (QY) is calculated by the equation $\Phi_x = \Phi_{st}(A_{st}/A_x)(F_x/F_{st})(\eta_x/\eta_{st})^2$, where Φ is the QY, A is the absorbency, F is the integal area of the fluorescence spectra, and η is the refractive index of the solvent. The subscrip "st" and "x" refers to standard that has known QY value and the sample to be tested, respectively. Using quinine sulfate (QY = 54%) as the reference, the QY of the synthesized CDs was calculated to be 23.27%, which is higher than most of the reported CDs.

3.1.2 Characterization of CDs/PAM composite hydrogel film. The results indicate that the prepared CDs/PAM composite hydrogel film was transparent under natural light (Fig. 4a) and emitted bright blue fluorescence under the ultraviolet light of 365 nm(Fig. 4b), which showed that the CDs were successfully compounded in the PAM hydrogel film. The freeze-dried CDs/PAM composite hydrogel film were observed by SEM. As

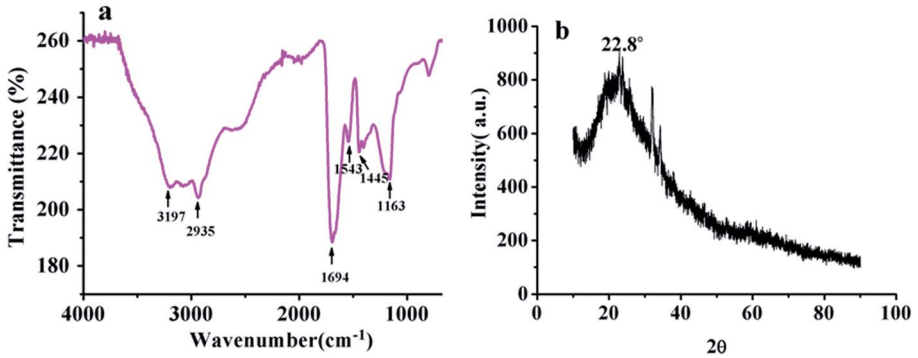

Fig. 2 Characterization of CDs by (a) FT-IR spectrum and (b) XRD pattern.

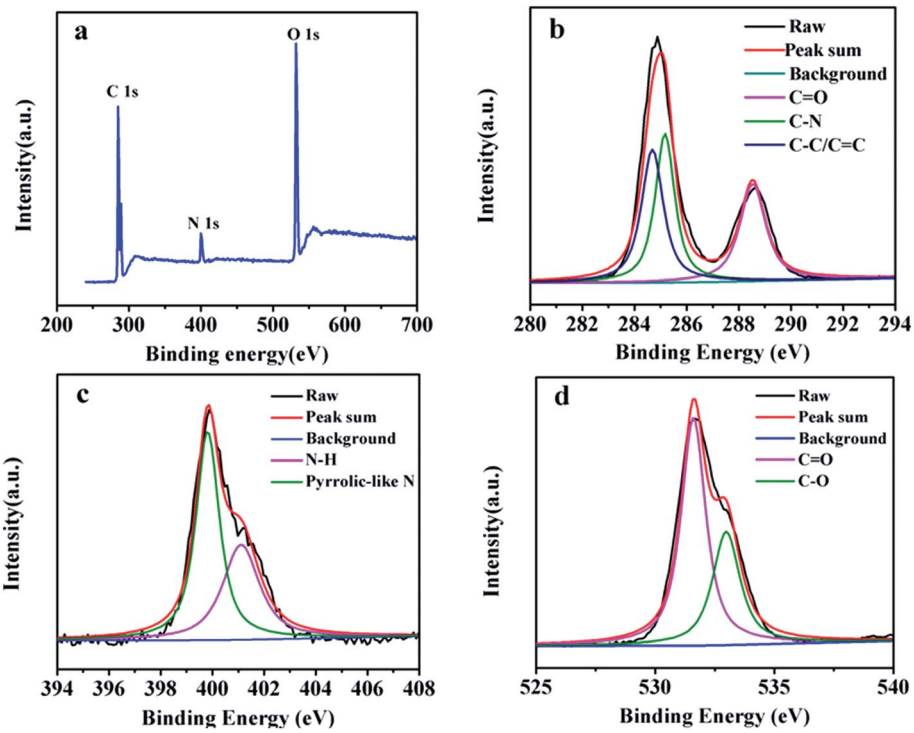

Fig. 3 Entire XPS scanning spectra of CDs (a); XPS high resolution survey scan of C 1s (b); XPS high resolution survey scan of N 1s (c); XPS high resolution survey scan of O 1s (d).

shown in Fig. 4c, the CDs/PAM composite hydrogel film exhibited a porous structure, indicating that water, ions and molecules can pass through the composite film freely.

3.2 Detection of ONZ with CDs/PAM composite hydrogel film

The preliminary experiment results indicate that the fluorescence of CDs/PAM composite hydrogel film can be quenched by ONZ aqueous solution. In order to further discuss the fluorescence quenching efficiency and optimize the sensor response to ONZ, test conditions including excitation wavelength, pH value, ion strength were investigated as followed.

3.2.1 Optimization of excitation wavelength. The fluorescence quenching efficiency equals $(F_0 - F)/F_0$, in which F_0 is the original fluorescence of the system, F is the fluorescence of the system after adding the substance to be measured. In order to maximize the ONZ's quenching efficiency to the CDs/PAM composite hydrogel film, the optimum excitation wavelength in the range of 300–370 nm was studied. As shown in Fig. 5a, the highest quenching efficiency was observed at the excitation wavelength of 320 nm. Therefore, 320 nm was selected as the optimal excitation wavelength for the following experiments.

3.2.2 Effects of pH value of solution on the detection of ONZ. The pH value of solution is an extremely important factor

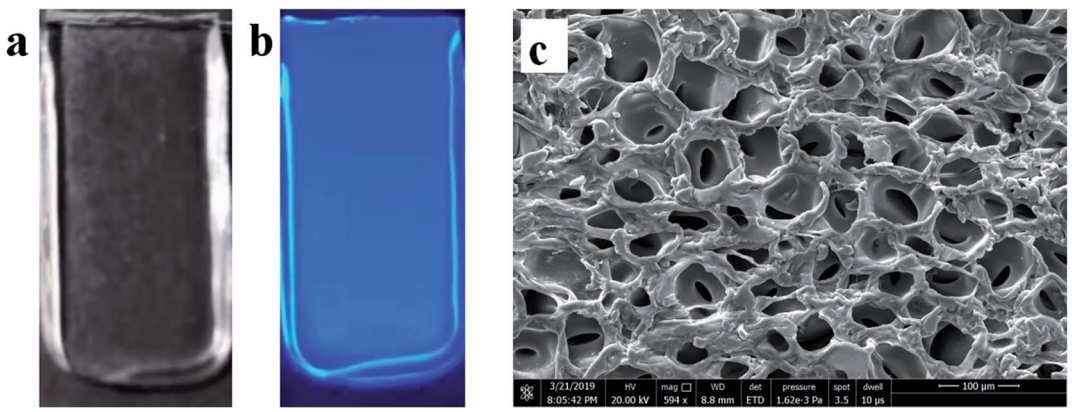

Fig. 4 Morphological and fluorescent characterization of CDs/PAM composite hydrogel film ((a): digital photos under natural light; (b): digital photos under 365 nm UV light; (c): SEM image).

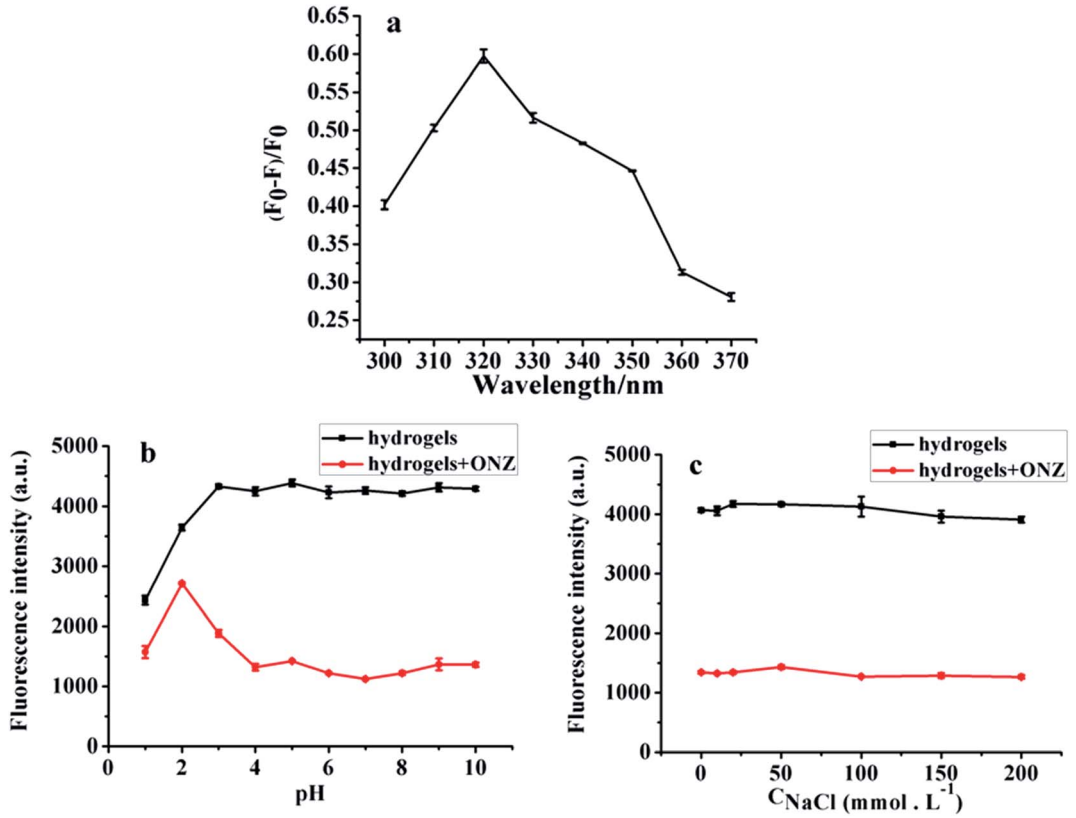

Fig. 5 Optimization of the experimental conditions for determination of ONZ (a): the quenching efficiency $(F_0 - F)/F_0$ of CDs/PAM composite hydrogel film for detection of ONZ at different excitation wavelengths; (b): effects of pH value of solution on the fluorescence intensity of blank composite hydrogel film and ONZ-composite hydrogel film; (c): effects of ionic strengths on fluorescence intensity of blank composite hydrogel film and ONZ-composite hydrogel film.

on the fluorescence quenching effects. Under the wavelength of 320 nm, the fluorescence intensity of the film was investigated in the blank and the ONZ contained test solution of a series of different pH value (1–10). As can be seen from Fig. 5b, the fluorescence intensity of the CDs/PAM composite hydrogel film, both in the blank and the ONZ contained test solution, tends to be stable after pH = 4, indicating that the suitable condition of solution for ONZ detection is from weakly acidic to alkaline. For stable detection of real samples and maximize the fluorescence quenching efficiency, pH of the solution is set as 7.

3.2.3 Effect of ionic strength on the detection of ONZ. The ionic strength is an important factor in the swelling process of the hydrogel film and fluorescence intensities of carbon dots.[42] The effect of ionic strength of solution on the detection of ONZ was investigated at room temperature. As shown in Fig. 5c, the fluorescence intensity of the composite hydrogel film in both blank and 80 μM ONZ test solution was slightly affected even when the concentration of NaCl increased to 200 mM. The result indicated that the CDs/PAM composite hydrogel film exhibited enough anti-interference capability against ions, suggesting that the CDs/PAM composite hydrogel film have certain advantages in further application.

3.2.4 Selectivity of CDs/PAM composite hydrogel film for detection of ONZ. The selectivity of CDs/PAM composite hydrogel film to ONZ is of great importance because of the complex components content and the diversity of the real environmental samples. Therefore, under the optimal detection conditions, the effect of cations (1.5 times of ONZ equivalents) such as Ca^{2+}, Cu^{2+}, Fe^{2+}, Fe^{3+}, Hg^{2+}, K^{+}, Na^{+}, Mg^{2+}, Zn^{2+}; anions (5 times of ONZ equivalents) such as F^{-}, Cl^{-}, SO_4^{2-}, CO_3^{2-}; amino acid molecules (5 times of ONZ equivalents) such as serine, lysine, histidine, glutamic acid; urea (5 times of ONZ equivalents) and glucose (5 times of ONZ equivalents) on the fluorescence intensity were investigated in detail. As can be seen from Fig. 6a, the existence of other interferents in blank aqueous solutions contributes slight change to the fluorescence intensity, while evident fluorescence quenching effect appears when ONZ exists in the solution, with and without other interferents, indicating that the fluorescence of CDs/PAM composite hydrogel film has good selectivity to ONZ.

3.2.5 Anti-interference capacity of CDs/PAM composite hydrogel film. To further investigate the anti-interference capacity of the CDs/PAM composite hydrogel film in the detection of ONZ, a series interference experiments were conducted to

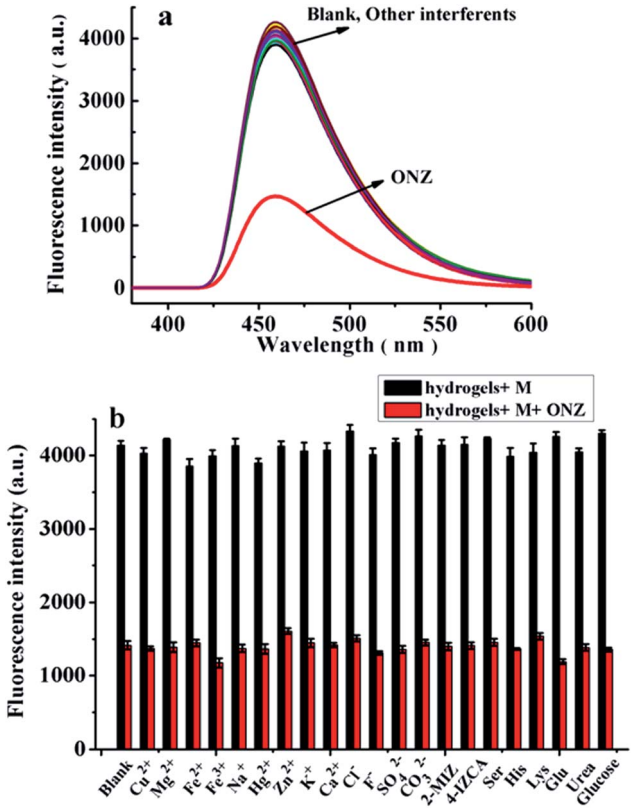

Fig. 6 Investigation of anti-interference capacity for detection of ONZ with CDs/PAM composite hydrogel film ((a): fluorescence spectra of ONZ and interferents detected by CDs/PAM composite hydrogel film; (b): effects of interferents on the fluorescence intensity of ONZ-composite hydrogel film).

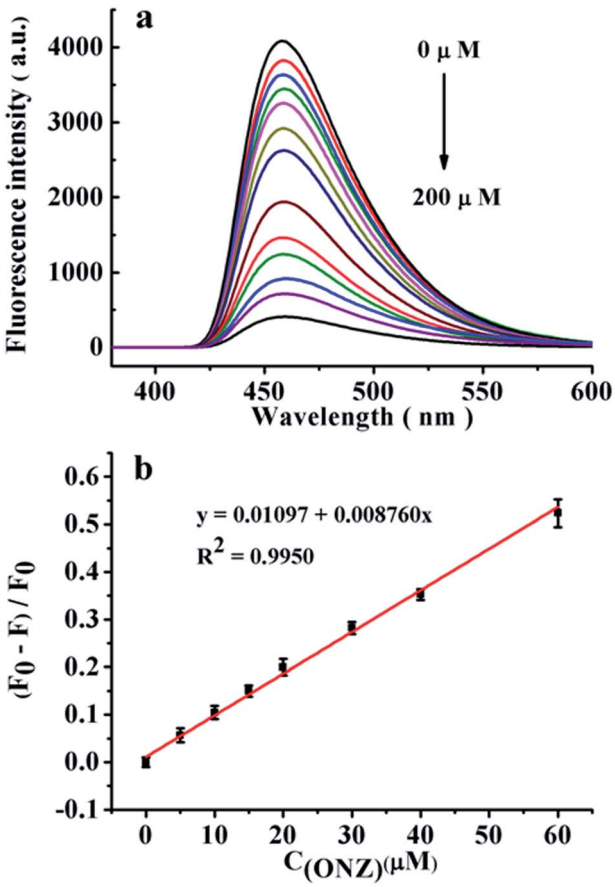

Fig. 7 Quantitative detection of ONZ by CDs/PAM composite hydrogel film (a): fluorescence spectra of different concentrations of ONZ detected by CDs/PAM composite hydrogel film; (b): the calibration line of quantitative detection of ONZ by CDs/PAM composite hydrogel film.

explore the influence of various interferents towards the detection of ONZ. Under the optimal detection conditions, the fluorescence intensity of the CDs/PAM composite hydrogel film with interferent solution, with and without ONZ, were determined. The interferents includes cations (1.5 times of ONZ equivalents) such as Ca^{2+}, Cu^{2+}, Fe^{2+}, Fe^{3+}, Hg^{2+}, K^{+}, Na^{+}, Mg^{2+}, Zn^{2+}; anions (5 times of ONZ equivalents) such as F^{-}, Cl^{-}, SO_4^{2-}, CO_3^{2-}; amino acid molecules (5 times of ONZ equivalents) such as serine, lysine, histidine, glutamic acid; urea (5 times of ONZ equivalents) and glucose (5 times of ONZ equivalents). As shown in Fig. 6b, the results indicate that the existence of ONZ in all interferent solutions have obvious fluorescence quenching effect on the CDs/PAM composite hydrogel film. This result clearly shows that the established method for detection of ONZ exhibits strong anti-interference capacity and high accuracy, which can be used for the detection of ONZ in complex matrix samples.

3.2.6 Quantitative detection of ONZ by CDs/PAM composite hydrogel film. In order to explore the possibility of quantitative detection of ONZ by using CDs/PAM composite hydrogel film, a series of ONZ solution with different concentration (0, 5, 10, 15, 20, 30, 40, 60, 80, 100, 120, 150, 200 μM) were prepared and the fluorescence emission spectra of the film were recorded. As can be seen from Fig. 7a, the fluorescence intensity of CDs/PAM composite hydrogel film decreased gradually with the increase of ONZ concentration. And in Fig. 7b, the linear relationship ($y = 0.01097 + 0.008760x$) between the fluorescence quenching efficiency ($(F_0 - F)/F_0$) and the concentration of ONZ was good ($R^2 = 0.9950$) in the ONZ concentration range of 5–60 μM, with the LODs of 2.35 μM ($3\sigma/k$).

3.2.7 Investigation of repeatability and stability of CDs/PAM composite hydrogel film. In order to explore the reusability of CDs/PAM composite hydrogel film for the detection of ONZ, the same CDs/PAM composite hydrogel film was used in this study for repetitive experiments. Firstly, the fluorescence of CDs/PAM composite hydrogel film with blank solution and 100 μM ONZ solution were measured subsequently. And then the CDs/PAM composite hydrogel film was immersed in a 20% ethanol aqueous solution to remove the ONZ and then subjected to spectral test. As shown in Fig. 8a, the CDs/PAM composite hydrogel film exhibited good responsiveness to ONZ after repeating 6 cycles. It can be seen that the CDs/PAM composite hydrogel film prepared by this method has the characteristics of recycling and reuse.

Meanwhile, to explore the stability performance of the obtained CDs/PAM composite hydrogel film, the CDs/PAM composite hydrogel film was refrigerated for 0, 5, 10, 15,

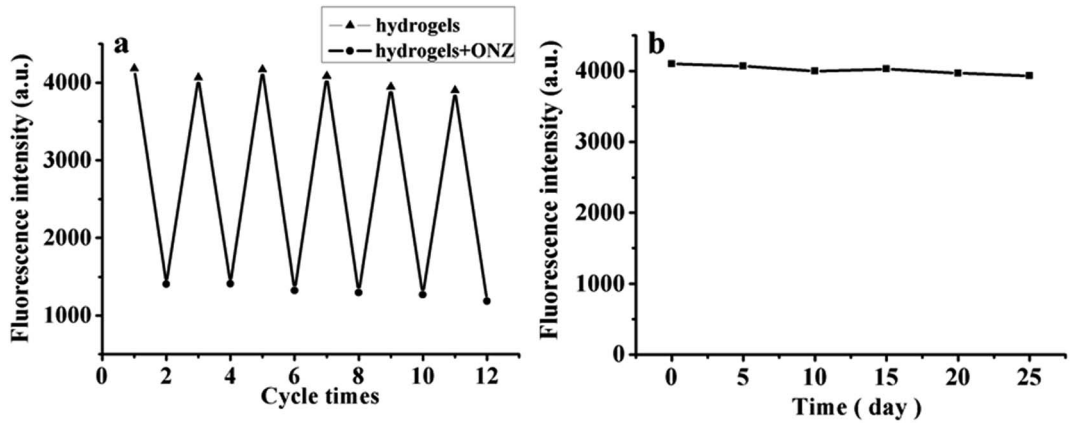

Fig. 8 Investigation of repeatability (a) and preservation stability (b) of CDs/PAM composite hydrogel film.

20 and 25 days, and the fluorescence intensity of the film was measured by fluorescence emission spectroscopy. As shown in Fig. 8b, the fluorescence intensity of CDs/PAM composite hydrogel film remained almost unchanged during storage, indicating that the CDs/PAM composite hydrogel film possesses sufficient stability.

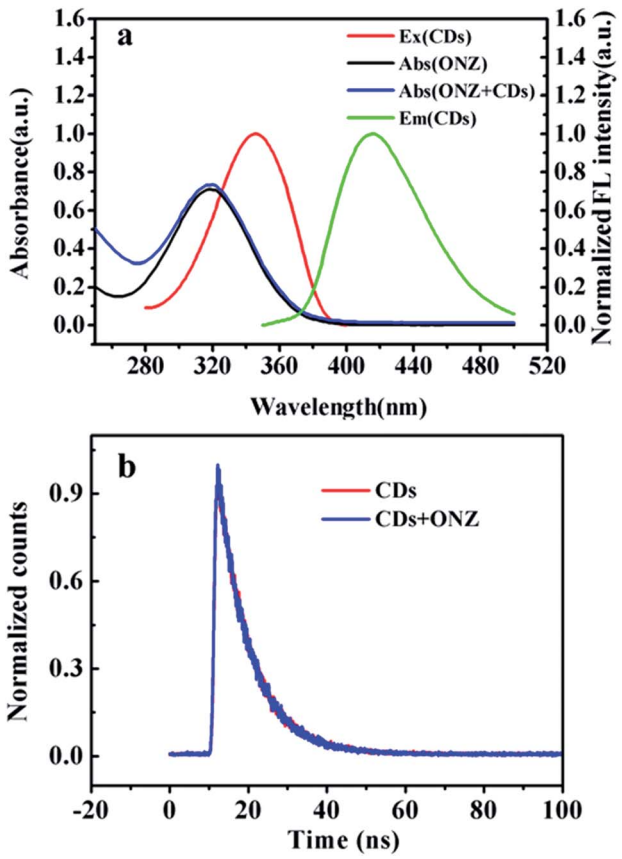

Fig. 9 Investigation of the quenching mechanism (a): the fluorescence excitation spectrum, emission spectrum of CDs, and the UV-vis absorption spectrum of ONZ; (b): fluorescence decay of CDs without and with ONZ.

Table 1 Recoveries of detection of ONZ in ONZ dispersible tablets and urine

Sample	Concentration taken/μM	Found/μM	Recovery/%	RSD/%
Urine	0	—	—	—
	15	14.18	94.53	6.2
	25	24.28	97.12	1.7
	50	50.87	101.7	2.1
Ornidazole dispersion tablets	0	7.41	—	—
	7	14.46	96.40	1.4
	17	25.57	102.3	2.0
	42	46.12	92.24	2.7

3.2.8 Possible quenching mechanism of ONZ towards CDs/PAM composite hydrogel film. In order to explore the possible quenching mechanism of ONZ towards CDs/PAM composite hydrogel film, the ultraviolet absorption spectra of ONZ, the fluorescence excitation and emission spectra of CDs were investigated in detail. As shown in Fig. 9a, the UV adsorption peak of ONZ was at 318 nm and remained almost unchanged when the CDs were added, indicating that no new complex was formed between CDs and ONZ. And the excitation peak of the CDs has some part overlapped with the ultraviolet absorption peak of ONZ. Based on these results, we speculated that the quenching mechanism may be caused by the internal filtration effect (IFE) between CDs and ONZ. To verify the conjecture, the fluorescence lifetime of CDs with or without ONZ was measured. As shown in Fig. 9b, the fluorescence lifetime after fitting is at 8.38 ns and 8.31 ns, respectively, which suggested that the fluorescence lifetime remain unchanged. Therefore, it was further proved that the quenching mechanism was caused by IFE.[43–47]

3.2.9 Application in actual samples detection. In order to explore the feasibility of the method in practical application, a recovery experiment was carried out using the human urine and dispersible tablets. As shown in Table 1, the

recoveries of ONZ detected by the CDs/PAM composite hydrogel film was between 92.24% and 102.3% and the relative standard deviation was below 10%. Therefore, the obtained CDs/PAM composite hydrogel film provided a fast and accurate method for detection of ONZ in a certain concentration range.

4. Conclusion

In this study, a novel CDs/PAM composite hydrogel film with good fluorescence performance was successfully prepared by using anhydrous citric acid and acrylamide as carbon sources and PAM hydrogel as the precursor liquid crosslinker. The obtained CDs/PAM composite hydrogel film exhibited good fluorescence quenching effect with high selectivity on ONZ. The prepared CDs/PAM composite hydrogel film show good performance in quantitative detection of ONZ, with a good liner relationship between the fluorescence quenching efficiency and the concentration of ONZ in the ONZ concentration range of 5–60 μM, with the LODs of 2.35 μM ($3\sigma/k$). The prepared CDs/PAM composite hydrogel film was also applied to detect ONZ in real samples such as ONZ dispersible tablets and urine with satisfactory recoveries. Furthermore, the CDs/PAM composite hydrogel film exhibited good stability, and can be recycled and reused for many times. Therefore, the obtained CDs/PAM composite hydrogel film is an environment-friend material for repeatable, high-efficient and sensitive detection of ONZ.

Conflicts of interest

There are no conflicts to declare.

Acknowledgements

This work was supported and sponsored by the National Natural Science Foundation of China (21677053, 21876033).

References

1 H. J. Wang, D. Qian, X. Xiao, B. He, S. Gao, H. Shi and J. Deng, *Electrochim. Acta*, 2017, **246**, 338–347.
2 P. Rajesh, S. Gunasekaran and T. Gnanasambandan, *Spectrochim. Acta, Part A*, 2016, **153**, 496–504.
3 M. Mehrzad Samarin, F. Faridbod and M. R. Ganjali, *Spectrochim. Acta, Part A*, 2019, **206**, 430–436.
4 L. Zhao, J. Y. Li, Y. Li, T. G. Wang, X. L. Jin, K. Wang, E. Rahman, Y. Xing, B. J. Ji and F. Zhou, *Food Chem.*, 2017, **229**, 439–444.
5 H. W. Sun, F. C. Wang and L. F. Ai, *J. Chromatogr. B: Anal. Technol. Biomed. Life Sci.*, 2007, **857**, 296–300.
6 P. N. Ranjane, S. V. Gandhi, S. S. Kadukar and K. G. Bothara, *J. Chromatogr. Sci.*, 2010, **48**, 26–28.
7 J. B. Du, Z. Y. Ma, Y. F. Zhang, T. Wang, X. Y. Chen and D. F. Zhong, *J. Pharm. Biomed. Anal.*, 2013, **86**, 182–188.
8 M. D. Konieczynska and M. W. Grinstaff, *Acc. Chem. Res.*, 2017, **50**, 151–160.
9 X. X. Wang, Q. Li, Y. Guan and Y. J. Zhang, *Mater. Today Chem.*, 2016, **1–2**, 7–14.
10 H. L. Luo, J. J. Dong, F. L. Yao, Z. W. Yang, W. Li, J. Wang, X. H. Xu, J. Hu and Y. Z. Wan, *Nano-Micro Lett.*, 2018, **10**(3), 42.
11 Z. L. Li, M. Tang, J. W. Dai, T. S. Wang and R. K. Bai, *Polymer*, 2016, **85**, 67–76.
12 G. Sharma, B. Thakur, M. Naushad, A. Kumar, F. J. Stadler, S. M. Alfadul and G. T. Mola, *Environ. Chem. Lett.*, 2017, **16**, 113–146.
13 S. Y. Lim, W. Shen and Z. Q. Gao, *Chem. Soc. Rev.*, 2015, **44**, 362–381.
14 Q. Wang, Z. Z. Feng, H. He, X. Hu, J. Mao, X. L. Chen, L. H. Liu, X. Y. Wei, D. Liu, S. M. Bi, X. J. Wang, B. S. Ge, D. Y. Yu and F. Huang, *Chem. Commun.*, 2021, **57**(45), 5554–5557.
15 Y. Z. Shen, T. T. Wu, Y. Q. Wang, S. L. Zhang, X. L. Zhao, H. Y. Chen and J. J. Xu, *Anal. Chem.*, 2021, **93**(8), 4042–4050.
16 B. Y. Zhang, Q. Q. Duan, H. C. Zhao, Y. X. Zhang, X. N. Li, Y. F. Xi, Z. F. Wu, L. Guo, P. C. Li and S. B. Sang, *Sens. Actuators, B*, 2021, **329**, 129156, DOI: 10.1016/j.snb.2020.129156.
17 X. C. Yang, Q. L. Li, M. Tang, Y. L. Yang, W. Yang, J. F. Hu, X. L. Pu, J. L. Liu, J. T. Zhao and Z. J. Zhang, *ACS Appl. Mater. Interfaces*, 2020, **12**(18), 20849–20858, DOI: 10.1021/acsami.0c02206.
18 H. J. Qi, C. Shi, X. N. Jiang, M. Teng, Z. Sun, Z. H. Huang, D. Pan, S. X. Liu and Z. H. Guo, *Nanoscale*, 2020, **12**(37), 19112–19120, DOI: 10.1039/d0nr02965c.
19 Z. T. Zhang, G. Y. Yi, P. Li, X. X. Zhang, H. Y. Fan, Y. L. Zhang, X. D. Wang and C. X. Zhang, *Nanoscale*, 2020, **1226**, 13899–13906, DOI: 10.1039/d0nr03163a.
20 H. F. Wu and C. L. Tong, *Anal. Chem.*, 2020, **92**(13), 8859–8866, DOI: 10.1021/acs.analchem.0c00455.
21 M. Bhatt, S. Bhatt, G. Vyas, I. H. Raval, S. Haldar and P. Paul, *ACS Appl. Nano Mater.*, 2020, **3**(7), 7096–7104, DOI: 10.1021/acsanm.0c01426.
22 B. Peng, M. M. Fan, J. M. Xu, Y. Guo, Y. J. Ma, M. Zhou, J. L. Bai, J. F. Wang and Y. J. Fang, *Microchim. Acta*, 2020, **187**(12), 660, DOI: 10.1007/s00604-020-04641-9.
23 J. An, R. B. Chen, M. Z. Chen, Y. Q. Hu, Y. Lyu and Y. F. Liu, *Sens. Actuators, B*, 2021, **329**, 129097, DOI: 10.1016/j.snb.2020.129097.
24 X. C. Li, S. J. Zhao, B. L. Li, K. Yang, M. H. Lan and L. T. Zeng, *Coord. Chem. Rev.*, 2021, **431**, 213686, DOI: 10.1016/j.ccr.2020.213686.
25 Y. H. Zhang, K. Zhou, Y. Qiu, L. Xia, Z. N. Xia, K. L. Zhang and Q. F. Fu, *Sens. Actuators, B*, 2021, **339**, 129922, DOI: 10.1016/j.snb.2021.129922.
26 X. Y. Tang, Y. M. Liu, X. L. Bai, H. Yuan, Y. K. Hu, X. P. Yu and X. Liao, *Anal. Chim. Acta*, 2021, **1157**, 338394, DOI: 10.1016/j.aca.2021.338394.
27 J. H. Zheng, R. M. Zhang, X. G. Wang and P. F. Yu, *J. Mater. Sci.*, 2019, **54**, 13509–13522.
28 A. Konwar, N. Gogoi, G. Majumdar and D. Chowdhury, *Carbohydr. Polym.*, 2105, **115**, 238–245.

29 H. Yang, L. He, S. Pan, H. Liu and X. Hu, *Spectrochim. Acta, Part A*, 2019, **210**, 111–119.
30 G. L. Liu, Z. Chen, X. Y. Jiang, D. Q. Feng, J. Y. Zhao, D. H. Fan and W. Wang, *Sens. Actuators, B*, 2016, **228**, 302–307.
31 G. F. Guo, L. Y. Yu, B. Y. Zhu, M. Y. Tang, F. Chai, C. G. Wang and Z. M. Su, *RSC Adv.*, 2018, **8**, 16095–16102.
32 Y. Q. Wang, Y. N. Xue, S. R. Li, X. H. Zhang, H. X. Fei, X. G. Wu and W. Y. Chen, *J. Polym. Res.*, 2017, **24**, 224–230.
33 M. Hu, X. Gu, Y. Hu, T. Wang, J. Huang and C. Y. Wang, *Macromolecules*, 2016, **49**, 3174–3183.
34 J. M. Ma, G. Y. Zhou, L. Chu, Y. T. Liu, C. B. Liu, S. G. Luo and Y. F. Wei, *ACS Sustainable Chem. Eng.*, 2016, **5**, 843–851.
35 M. Picard, S. Thakur, M. Misra and A. K. Mohanty, *RSC Adv.*, 2019, **9**, 8628–8637.
36 M. Chen, W. Wu, Y. Y. Chen, Q. P. Pan, Y. Z. Chen, Z. F. Zheng, Y. J. Zheng, Y. L. Huang and S. H. Weng, *RSC Adv.*, 2018, **8**, 41432–41438.
37 Y. Jiao, X. J. Gong, H. Han, Y. F. Gao, W. J. Lu, Y. Liu, M. Xian, S. M. Shuang and C. Dong, *Anal. Chim. Acta*, 2018, **1042**, 125–132.
38 F. F. Du, X. J. Gong, W. J. Lu, Y. Liu, Y. F. Gao, S. M. Shuang, M. Xian and C. Dong, *Talanta*, 2018, **179**, 554–562.
39 J. X. Zheng, J. L. Wang, Y. L. Wang, Y. Z. Yang, X. G. Liu and B. S. Xu, *J. Electron. Mater.*, 2018, **47**, 7497–7504.
40 Y. Zhang, Z. Y. Gao, X. Yang, G. Q. Yang, J. L. Chang and K. Jiang, *RSC Adv.*, 2019, **9**(11), 6084–6093.
41 Y. B. Liu, D. Y. Chao, L. Zhou, Y. N. Li, R. P. Deng and H. J. Zhang, *Carbon*, 2018, **135**, 253–259.
42 A. Alam, Y. J. Zhang, H. C. Kuan, S. H. Lee and J. Ma, *Prog. Polym. Sci.*, 2018, **77**, 1–18.
43 Z. Han, Y. W. Long, S. Pan, H. Liu, J. D. Yang and X. L. Hu, *Anal. Methods*, 2018, **10**, 4085–4093.
44 L. Han, S. G. Liu, J. Y. Liang, Y. J. Ju, N. B. Li and H. Q. Luo, *J. Hazard. Mater.*, 2019, **362**, 45–52.
45 Y. N. Zhao, S. Y. Zou, D. Q. Huo, C. J. Hou, M. Yang, J. J. Lia and M. H. Bian, *Anal. Chim. Acta*, 2019, **1047**, 179–187.
46 Q. Q. Zhang, B. B. Chen, H. Y. Zou, Y. F. Li and C. Z. Huang, *Biosens. Bioelectron.*, 2018, **100**, 148–154.
47 Y. J. Ma, Y. Y. Song, Y. S. Ma, F. D. Wei, G. H. Xu, Y. Cen, M. G. Shi, X. M. Xu and Q. Hu, *New J. Chem.*, 2018, **48**, 8992–8997.